Core Ideas

- Modeled ETo gradients present variations as a function of altitude, annual cycle, and total amount.
- A very good match between different soil moisture monitoring devices has been achieved.
- Groundwater level monitoring revealed dominant hydrodynamic evolution mechanisms.
- Hydrochemical monitoring supports groundwater hydrology findings and reveals pollution sources.
- Monitoring the PHO supports accurate hydrologic modeling and sustainable water use.

V. Pisinaras, A. Panagopoulos, C. Doulgeris, A. Ilias, and E. Tziritis, Soil & Water Resources Institute, Hellenic Agricultural Organization "DEMETER," 57400 Thessaloniki, Greece; F. Herrmann, H.R. Bogena, and F. Wendland, Agrosphere Institute (IBG-3), Forschungszentrum Jülich, 52425 Jülich, Germany. *Corresponding author (f.wendland@fz-juelich.de).

Hydrologic and Geochemical Research at Pinios Hydrologic Observatory: Initial Results

Vassilios Pisinaras, Andreas Panagopoulos, Frank Herrmann, Heye R. Bogena, Charalampos Doulgeris, Andreas Ilias, Evangelos Tziritis, and Frank Wendland*

The Pinios Hydrologic Observatory (PHO) is located in the River Pinios basin, which is one of the most productive basins in Greece. The PHO was established to develop deep knowledge of water balance at the river basin scale and to improve understanding of the major hydrodynamic mechanisms to improve hydrological modeling and ultimately sustainable water resource management. The PHO comprises three meteorological stations, 12 groundwater monitoring sites, and one soil moisture monitoring site, which includes frequency domain reflectometry sensors (SoilNet) and a cosmic-ray neutron sensor (CRNS) probe. Although the PHO was recently established (at the end of 2015), the preliminary findings from data analysis are promising. Calculated reference evapotranspiration (ETo) gradients demonstrate differences regarding their annual cycle, total amount, and altitude level. Moreover, climate analysis indicates nocturnal mountain-valley winds. Groundwater level spatial distribution indicates the dominant recharge mechanisms to the alluvial aquifer system. These findings are also supported by the hydrochemical data analysis (electrical conductivity and, secondarily, NO_3 distribution). Locally elevated NO_3 concentrations are attributed to agricultural activities and call for review of the adopted farming practices. Results from the soil moisture monitoring site indicate a very good match between the CRNS probe and the average SoilNet data. Future perspectives of the PHO include geophysical surveys to accurately delineate the geometry of the groundwater system, the expansion of groundwater and soil moisture observation networks, and the application of the mGROWA hydrologic model to accurately simulate the hydrological processes in the PHO and upscale in the entire River Pinios basin. Finally, in support of the local farmers, we plan to develop and implement a distributed irrigation programming protocol in the entire area of the PHO.

Abbreviations: CRNS, cosmic-ray neutron sensor; CS, Climate Station; EC, electrical conductivity; ET, actual evapotranspiration; ETo, reference evapotranspiration; PHO, Pinios Hydrologic Observatory; RPB, River Pinios basin; TR, total runoff.

Efficient water resources management is of critical importance to sustain anthropogenic activities and preserve ecological functions, especially in the water-stressed southern European belt and the circum-Mediterranean region in which climate change impacts are expected to be severe (Bangash et al., 2013; Chenoweth et al., 2011; García-Ruiz et al., 2011; Milano et al., 2013). The profound uneven spatiotemporal distribution of precipitation and the ever-increasing water demands to sustain economic activities of all sectors of the industry often lead to water shortages, overexploitation of available reserves, and water quality deterioration (Milano et al., 2013; Roson and Sartori, 2010). The United Nations, through the 17 Sustainable Development Goals, prioritize rational water resources management (United Nations, 2015), and the European Commission has developed a comprehensive toolbox to support and impose sustainable water resources management (Water Framework Directive 2000/60/EC, Groundwater Directive 2006/118/EC, Nitrates Directive 91/676/EEC). Water governance strategies have also

been developed to this end. These tools are based on the compilation of specific water resources management plans at the river basin scale that incorporate suites of measures tested for their efficacy and appropriateness with the aid of mathematical models.

The effectiveness of the compiled measures relies on the accuracy of the characterization and assessment of water systems and the reliability of the compiled models, which in turn depend on the quality, adequacy, frequency, representativeness, and length of available hydrological and hydrogeological data. In several cases, a lack of sufficient data and/or data of low reliability is common and impedes any attempt to manage available water resources in a sustainable and efficient manner.

The River Pinios basin (RPB), located in the central part of Greece, is a typical case of a basin were data availability partially enables assessment of the current status and evolution of water resources. However, it does not allow development of a deep understanding and quantification of key hydrodynamic mechanisms and systematic observation of water quality characteristics. Due to this shortfall, modeling exercises may lack accuracy and reliability. The RPB has a spatial extent of $\sim$11,000 km^2 and is one of the most productive areas of the country. More than 80% of the total fresh water consumption in the basin is used for irrigation, predominantly through a dense network of wells and surface water resources directly abstracted from River Pinios, its tributaries, and numerous karstic springs that emerge at the margins of the plains. Groundwater overexploitation and quality deterioration triggered by prolonged droughts and poor management practices in the mid-1980s is well documented (e.g., Alexandridis et al., 2014; Hellenic Special Secretariat for Water, 2012; Kaplanidis and Fountoulis, 1997; Marinos et al., 1997; Panagopoulos, 1995, 1996) and jeopardizes regional socio-economic stability and growth in the future. Efficient and sustainable water and soil resources management, especially in view of climate change impacts, is therefore of paramount importance to ensure water sufficiency and to safeguard food security for the future.

Since 2000, most of the RPB has been declared as being sensitive to NO$_3$ pollution originating from agricultural regions (Karyotis et al., 2002). In 2017, the reviewed water resources management plan at the river basin scale was compiled incorporating a suite of specific management measures (Hellenic Special Secretariat for Water, 2017). However, there are unanswered questions regarding the management options to effectively preserve water and soil resources of the basin and to efficiently manage water availability on the basis of natural recharge occurrence and water production to sustain irrigated agriculture along with domestic and other uses in the region. Water management authorities and stakeholders are thus posing pressing questions, such as:

1. Will there be enough water reserves to sustain demands, including those associated with agricultural production?
2. How will drought episodes affect water reserves, and what are the best management practices to sustain soil and water resources?
3. To what extent will a decrease in natural recharge affect groundwater reserves in terms of quantity and quality, and will there be irreversible damage caused to soil resources?

4. Can we support water governance through a decision support system only on the basis of existing monitoring data?

To answer stakeholders' practical questions, such as those presented above, and the science questions presented below, the agriculture- and hydrology-oriented Pinios Hydrologic Observatory (PHO) was established in 2015. The PHO belongs to the International Long Term Ecological Research Network established in 1993 and represents over 700 long-term ecological research sites (Mirtl et al., 2018).

Here we (i) explain the motivation of establishing the PHO; (ii) describe basic characteristics of the PHO and the existing instrumentation; (iii) describe the advancements made through the establishment and operation of the PHO, including preliminary insights about evapotranspiration, water balance, soil water content, and groundwater quantity and quality; and (iv) present future perspectives for the utilization and expansion of the PHO.

◦Motivation

In response to some of the aforementioned questions, a number of water balance models have been applied in the RPB or in its sub-basins (e.g., Koukidou and Panagopoulos, 2010; Pikounis et al., 2003; Psomas et al., 2016). These researchers applied the fully distributed, semi-empirical GROWA model (Herrmann et al., 2015; Kunkel and Wendland, 2002; Panagopoulos et al., 2015, 2016) and the fully distributed deterministic mGROWA model (Panagopoulos et al., 2017), which enables spatiotemporal discretization of the soil zone hydrodynamic evolution. Although the application of the mGROWA model to other Mediterranean basins and beyond (Ehlers et al., 2016; Herrmann et al., 2016; Tetzlaff et al., 2015) produced accurate results, the outcome for the RPB remained questionable due to a lack of reliable model input data and profound knowledge about the hydrodynamic evolution mechanisms (pathways of groundwater recharge from the surrounding marginal aquifer systems into the basin). These problems, accompanied by other critical questions and issues, resulted in eight motives that led us to establish the PHO.

Motive 1: Lack of Detailed and Accurate Daily Reference Evapotranspiration Values across the Entire Basin and Its Altitudinal Gradient

Evapotranspiration constitutes one of the most crucial water budget factors in Mediterranean basins because it is the major water sink. In hydrological modeling practice and in the mGROWA model, actual evapotranspiration (ET) is often calculated based on reference evapotranspiration (ETo) under consideration of vegetation-specific functions and parameters. Reference evapotranspiration is commonly calculated for a grass-covered reference surface using only observed climate variables (e.g., near-surface air temperature, wind speed, humidity). Whereas the network of precipitation stations in RPB is relatively dense, the density of the climate station network is low. Additionally, it shows significant data gaps, and, except for precipitation, the only available climate variable on a daily basis is temperature. This situation

hampers the computation of consistent and reliable gridded fields of temperature and ETo on a daily basis, which are, in addition to precipitation, the main climatic drivers of hydrologic models. This shortcoming compromises water budget calculations because crop water requirements, which account for 80% of the annual water demands at the regional level, may not be accurately approximated.

The most important precondition for a successful assessment of ETo is the availability of the full range of measurable climate variables in a small representative pilot area that is embedded in a larger model domain. Against this background, the climate stations installed in the PHO at different altitudes but relatively close to each other support the derivation of reliable ETo values for the whole RPB.

Motive 2: Missing Parameters with Relation to Calculation of Actual Evapotranspiration

Significant parts of the mountain ranges and their transition zone to the basin are coved by Mediterranean scrubland, suggesting that evapotranspiration, and thus runoff formation processes in the transition zone, are significantly controlled by this vegetation type, as they are by the soil water storage capacity of the prevailing Leptosol soils. Ehlers et al. (2016) emphasized that comprehensive modeling studies dealing with soil moisture and evapotranspiration of Mediterranean scrublands are rare. Thus, a solid and well-proven parameter set to determine ET rates with the mGROWA model is lacking for these site conditions and vegetation types. Against this background, the soil moisture observations in the PHO are intended to contribute calibration data for those site conditions. Because ET is not measured directly in the PHO, we plan to derive evapotranspiration fluxes from measured fluctuation patterns of soil moisture.

Motive 3: Lack of Justified Quantification of Major Hydrodynamic Evolution Mechanisms

In the RPB and in the PHO, significant amounts of water are transported laterally from the mountainous regions as surface and subsurface runoff to the aquifers of the basins (Panagopoulos et al., 2015). Based on the detailed knowledge of the geometry and the hydrogeology of the RPB, which is controlled by active fault tectonics, the dominant controlling mechanism of groundwater recharge is the lateral crossflow from surrounding marginal aquifer systems to the main alluvial systems of the basin. In most cases, crossflow is enhanced by a favorable hydraulic properties transition zone that is formed of coarse material in the form of talus cones and/or scree, depending on the location across the basin. Even though the occurrence and importance of this mechanism across the respective transition zone are identified and acknowledged, no detailed quantification has been accomplished.

Motive 4: Upscaling of Hydrodynamic Evolution Mechanisms and Hydrological Cycle Elements to Larger Scales

Studying in detail the hydrodynamic evolution mechanisms described above in a limited-size, well-controlled basin

that resembles the characteristics and properties of the core part of the RPB would enable developing deep understanding and quantification. Hence, the primary vision for the PHO is to serve as a pilot/model basin to study in detail under "controlled" conditions and to quantify the hydrological cycle elements and hydrodynamic evolution mechanisms that will then be transferred to regional scales.

Motive 5: Implementation of High Spatial Resolution and/or Frequency Monitoring in Water Budgeting and Advanced Hydrologic Data Analysis

High-frequency data series obtained from a dense network of high-resolution groundwater level and electrical conductivity (EC) sensors, coupled with water abstraction loggers, would provide information regarding the response of the groundwater system to natural recharge and the stress imposed during the summer peak water demand periods and would provide detailed calculations of hydraulic properties and groundwater flows. In conjunction with detailed calculations of natural vegetation and evapotranspiration evolution of cultivated crops over the year and throughout the altitudinal range of such a basin, through the analysis of high-frequency raw data collected from fully equipped climate stations, detailed water budget estimates could be made .

Motive 6: Development of Efficient and Innovative Water Management Strategies and Transfer to Larger Scales

In-depth study of processes taking place at the agrosphere zone in a predominantly agricultural environment is extremely important to understand the interactions between the atmosphere, crops, soil, water, and geological formations, especially regarding one of the dominant production areas of the country. It is believed that, through developing a deep understanding of such interactions and quantifying them, improved management and protection of available natural resources would be enabled. Having accomplished this task in a representative agricultural basin of the country, it was envisaged that lessons learned and management methodologies developed may be transferred to larger scales of the same and neighboring basins.

Motive 7: Development of Services for Stakeholders and the General Public

Numerous services to the scientific community and predominantly to the local society are envisaged through the long-term operation of the observatory, thus linking research to community. These include irrigation programming, rationalized management of available water resources through accurate calculations of annual recharge water volumes, drought management, soil preservation, approximation of the hydraulic properties of groundwater systems to better design and operate abstraction works, proactive plant protection, and efficient forest-fire risk management through the analysis of climate station monitoring data.

Motive 8: Development and Operation of Multiscale Monitoring Networks and Big Data Analysis

Detailed instrumented monitoring of key parameters that control the hydrologic evolution and balance is among the key drivers of compiling the PHO. Developing deep knowledge on big data management and efficient long-term operation management of such networks is a key target. Experience gained from this exercise is perceived as the foundation to expand instrumented telemetric monitoring across large basins and at a national scale. It is strongly believed that the success and long-term viability of such systems depend predominantly on the actual problem-solving they support and the level of dependence created to the local communities. In other words, for a monitoring system to be accepted and successful, it will have to prove its usefulness, and a dedicated group of users who depend on the produced data for concluding at least one function should be established. To this direction, the PHO, as of its primary stages of development, is fostered by the local municipality and by a group of dedicated farmers who guide the research group to their data needs and requirements and provide free access to their fields and farms for installation of necessary equipment.

Catchment Characteristics

The PHO is located at the eastern boundary of the RPB and covers an area of ~45 km^2 (Fig. 1a). According to the hydrolithological map presented in Fig. 1b, there are three dominant hydrolithological units identified in the PHO:

1. Fractured formations of low- to medium-permeability (HA2) are located at the northern mountainous part of the watershed and consist mainly of gneiss, gneiss-schists, and ultrabasic formations (amphibolites and prasinites). Within these units, groundwater flow occurs predominantly through their tectonically driven fractures (secondary porosity) and to a lesser extent through the primary porosity.
2. Alluvial deposits of variable permeability (HP1) consist mainly of recent deposits of variable texture, including lateral screes that fill the basin at the southern plain part of the PHO watershed in which a groundwater system of medium potential is formed.
3. Old talus cones and scree of variable permeability (HP4) favor direct infiltration of precipitation compared with the alluvia.

As previous hydrogeological studies have suggested (Hellenic Ministry of Agricultural Development and Food, 2012), lateral crossflows from the adjacent weathered crystalline rock formations at the northern parts of the basin (HA2) and the extensive transition zone that has developed along the same border of the basin (HP4) constitute the major groundwater recharge mechanism of the aquifer system that develops within the alluvium (HP1). Direct recharge through precipitation is important at the infiltration–transition zone (HP4) and occurs over the entire extent of the basin; however, its importance is reduced considerably there. The mountainous weathered crystalline rock formations (HA2) are not used for water production, and therefore no production wells exist in this system. Typically, this is the case in most of the margins of the entire RPB (i.e., mountainous groundwater systems characterized by discontinuities, such as fractures-fissures or karstic

conduits) and not primary porosity play an essential role to the recharge of the alluvial aquifers of the plains. The overexploitation of groundwater reserves, especially along the downstream southern part of the area, is indicated by the fact that the localized artesian phenomena reported in the past decades (Hellenic Ministry of Agricultural Development and Food, 2012) do not occur any longer, except for a limited number of cases and periods over exceptionally wet hydrological years. Several creeks confluence to a main stream flowing across the basin. This used to be a perennial stream that considerably contributed to groundwater recharge (Hellenic Ministry of Agricultural Development and Food, 2012); however, it is currently characterized by intermittent flow after significant precipitation events, during the snow-cover melting period, and during wet winters. Only limited groundwater discharge to the western–southwestern extent of the watershed occurs in the otherwise hydrologically secluded watershed, as reported previously (Hellenic Ministry of Agricultural Development and Food, 2012). Limited-extent karstified carbonate rocks crop out within the watershed; however, according to earlier hydrogeological studies, these are not hydraulically interconnected to formations outside the limits of this basin. Numerous springs emerge at the mountain front of the basin and are mostly used for agricultural purposes and domestic use. Most of them are ephemeral; however, a number of high-discharge perennial springs also occur. Overall, hydrogeological knowledge of the basin is limited; therefore, developing a deep understanding of aquifer geometry and hydrodynamics is a key driver for the PHO that will contribute greatly to the local community for efficient and sustainable water resources management.

Regarding land cover (Fig. 1c), the northern mountainous part of the watershed is dominated by mixed forests. Transitional woodland scrubs, broad-leaved forests, and natural grasslands also occur. This land cover is developed in a steep slope terrain, with altitude ranging between 400 and 1500 m. The southern plain part of the watershed, including the transition zone, is dominated by fruit trees, the most significant of which are apple (*Malus pumila* Mill.) and cherry (*Prunus* sp.). There are limited areas cultivated with annual crops, such as winter wheat (*Triticum aestivum* L.) and maize (*Zea mays* L.). Medium slopes are identified in the transition zone (altitude range 150–250 m), and low slopes are identified in the plain zone (altitude range 100–150 m) where the alluvial groundwater system occurs. Based on data retrieved from five soil profiles located in the plain zone of the PHO watershed, soils of sandy loam texture are dominant, although sandy clay loam and loamy soils have also been identified.

Regarding water resources management status, irrigation constitutes the major water consumer for the watershed, and demands are almost exclusively covered by groundwater. The majority of groundwater wells are private, although there is a small number of public groundwater wells operated by the Municipality of Agia through collective pressurized networks. Administratively, the PHO watershed constitutes part of Thessaly Water District (EL08) and is included in the RPB (EL0817). The PHO watershed is situated in the Almiros River surface water body
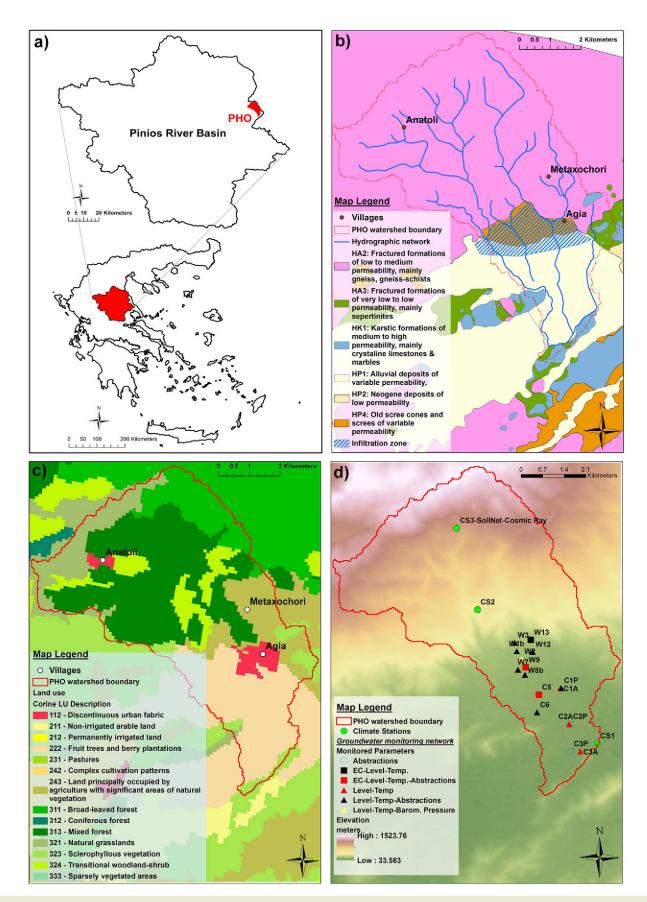
Fig. 1. Spatial information for the Pinios Hydrologic Observatory (PHO) watershed: (a) location map of the PHO in the River Pinios basin (RPB) and the RPB in Greece, (b) hydrolithological map, (c) land cover map according to CORINE classification, and (d) observation network distribution and digital elevation model.

(EL0816R000000163N) and in the Mavrovounio-Ossa ground-water body (EL0800270), the qualitative and quantitative status of which has been designated as good in the recently revised regional water management plans developed in the context of Water Framework Directive implementation. Nevertheless, according to Tziritis et al. (2016), agriculture constitutes a controlling factor for the hydrogeochemical conditions of the wider area, as reflected by the locally high NO_3 concentrations observed in the alluvial groundwater system. Moreover, the irrational irrigation practices applied in the area are reflected by locally increased salinization, which is attributed to irrigation water return flow. The salinity of applied fertilizers is being studied as another potential source of the identified issue.

⬥Pinios Hydrologic Observatory Installation Setup

Precipitation and Climate Observation Devices

The current basic observations setup in the PHO watershed is briefly described in Table 1. The spatial distribution of the network is presented in Fig. 1d. The PHO comprises three climate stations (Vaisala WXT520) in which precipitation, air temperature, air humidity, solar radiation, and wind speed and direction are monitored at a 10-min time interval. Climate Station (CS)1 was installed in October 2015 at an altitude of 152 m, CS2 was installed in November 2015 at 599 m, and CS3 was installed in April 2017 at 1031 m. Thus, a wide range of altitudes within the watershed is covered. In addition to the piezoelectric rainfall sensors installed at all three climate stations, weighing rain gauges (Pluvio[2], OTT) have been installed at CS1 and CS3 to ensure high-precision rainfall monitoring. A tipping bucket rain gauge (Rain-O-Matic Professional, Pronamic) has been installed in CS2 to compare rainfall amounts with the corresponding amounts

Table 1. Overview of basic monitoring parameters measured in the Pinios Hydrologic Observatory watershed.

Parameter	No. of monitoring sites/sensors	Recording time interval
		min
Climate		
Rainfall	3/6	10
Air temperature	3/3	10
Air humidity	3/3	10
Wind speed	3/3	10
Wind direction	3/3	10
Solar radiation	3/3	10
Snow depth	1/1	10
Groundwater		
Level	12/13	15
Temperature	12/13	15
Electric conductivity	3/3	15
Abstractions	11/11	10

from the piezoelectric sensor. All climate stations are telemetric and are equipped with logging facilities and zero-power modems that ensure low energy consumption despite the fact they are energy self-sustained through the use of electric circuitry driven by solar panels. A wind generator was installed at CS3, where a sonic snow depth sensor is also installed, to meet increased energy demands for antifrost protection of the station during winter, thus ensuring seamless and uninterrupted monitoring operation. Raw data collected from the climate stations are uploaded at frequent intervals on a dedicated web server and are made available to the involved research teams from Forschungszentrum Jülich Agrosphere Institute (IBG-3) and the Soil and Water Resources Institute of the Hellenic Agricultural Organization and to interested regional authorities, including the Municipality of Agia, the Regional Forestry Service, and the Regional Water Directorate. More details about data management are given below.

Soil Moisture Observation Devices

Soil moisture observation devices have been established around the area of CS3 (Fig. 1d), which comprises three SoilNet nodes (Bogena et al., 2010) implementing the Frequency Domain Reflectometry technology and one CRS-2000/B cosmic-ray neutron sensor (CRNS) probe (Hydroinnova LLC). Each SoilNet node comprises six SMT100 soil moisture sensors (Bogena et al., 2017) installed in pairs at 5, 20, and 50 cm soil depth, and the data recording interval is 15 min.

The CRNS probes detect fast neutron intensities produced by cosmic radiation, which are sensitive to soil moisture because they are strongly moderated by collisions with hydrogen nuclei (Bogena et al., 2015; Zreda et al., 2012). Therefore, soil moisture is inversely proportional to neutron intensity. Conversion of neutron intensity to soil moisture is described elsewhere (Andreasen et al., 2017; Desilets et al., 2010). The CRNS probe measures integral soil moisture in a circular footprint centered on the detector (radius range, 130–240 m) with penetration depths between 55 and 15 cm for soil moisture from 0.05 to 0.55 $cm^3\,cm^{-3}$ (Köhli et al., 2015; Schrön et al., 2017). The temporal resolution is 1 d. We used gravimetric samples taken within the CRNS footprint according to Schrön et al. (2017) to calibrate the CRNS probe.

The location of the SoilNet nodes and the CRNS probe accompanied by the approximate footprint area of the CRNS probe is presented in Fig. 2. In total, 90 gravimetric soil samples have been taken at 16 locations (from 0 to 30 cm depth in 5-cm increments) within the footprint of the CRNS probe. The irregular distribution of the sample locations is due to the steep topography, especially in the southeastern part of the CRNS footprint. Further soil sampling campaigns will be undertaken to better cover the whole footprint area. One of the SoilNet nodes and the CRNS probe were installed in the center of the small patch of low-sloped terrain covered by grass and herbs and very close to the CS3 climate station. The other two SoilNet nodes were installed underneath the scrubs surrounding the site (Fig. 2). The slope exposition of the CRNS footprint is to the south, and the

Fig. 2. Soil moisture observation site located at the high-altitude level of the Pinios Hydrologic Observatory (PHO) at 1031 m asl (yellow circle: climate station; blue circle: CRS-2000/B cosmic-ray neutron probe; red circles denote locations of the SoilNet nodes, each equipped with six SMT100 sensors; white crosses indicate locations of gravimetric samples). The 185-m circle indicates the approximate average footprint area of the cosmic-ray neutron sensor probe. (Satellite imagery: ESRI.)

slope angles are between 15 and 25°. The soil (Lithic Leptosol) shows highly variable rock contents and occasionally bare rock outcrops depending on the slope angle. Approximately 90% of the footprint area is covered by medium to high Mediterranean scrubland (Phrygana), and 10% is covered by grass and herbs.

Groundwater Observation Devices

The groundwater observation devices setup in the PHO watershed is briefly described in Table 1. After a detailed inventory of existing groundwater wells within the PHO watershed, a cluster of 12 groundwater monitoring stations was established, the spatial distribution of which is presented in Fig. 1d. Selection of monitoring wells was dictated by their spatial distribution to achieve the best possible spatial coverage of the alluvial groundwater system, focusing on the transition zone as its most critical part. All groundwater monitoring stations have been equipped with groundwater-level loggers of small size (DIVER micro-diver and mini-diver, Schlumberger Water Services) to obtain installation flexibility. The sensors' measuring range was carefully selected for each monitoring point according to well construction depth and groundwater level fluctuations, especially during abstractions, to maintain maximum accuracy. Three sites are additionally monitoring EC (CTD-DIVER, Schlumberger Water Services) to enhance the understanding of the hydrodynamic evolution mechanisms and to assist in quantification.

Another crucial parameter monitored is groundwater abstraction. This is achieved by installing pulse water abstraction meters in productive groundwater wells, accompanied by miniature loggers (OM-CP-PULSE101A, Omega Engineering). In the cases where groundwater level monitoring wells were not productive, the closest productive well was selected (satellite piezometer) to install the water abstraction meter (5–20 m apart). In this way, correlation of the monitoring wells to adjacent production wells enables the analysis of pumping test data, thus allowing for the derivation of reliable values for key hydraulic parameters of the groundwater system. Furthermore, analysis of groundwater level fluctuations within the productive groundwater well enables calculations of the well efficiency of the related wells, which in turn allows for better calculations of appropriate groundwater abstraction rates and overall management of available resources and pumping equipment in a way to maximize efficiency and reduce energy consumption. At C1, sensors monitoring groundwater level and temperature have been installed on both the productive well and the nearest satellite well. Moreover, by correlating groundwater abstractions to the irrigated areas, irrigation water management will be investigated and assessed, which is crucial because no relevant data are available.

Groundwater monitoring sites established in the PHO can be distinguished in two well-defined groups. The first group of monitoring sites, flagged as "W," is situated in the transition zone and was installed in December 2015. The second group, flagged as "C," is situated in the alluvial zone (Fig. 1d) and was installed in April 2017. Both groups sufficiently cover groundwater monitoring in the aforementioned hydrolithological units, and their spatial distribution enables calculation of transmissivities and compilation of piezometric maps. The density of monitoring sites established in the transition zone is higher due to the higher hydraulic slopes indicated in this unit and its importance in the hydrodynamic evolution of the alluvial groundwater system. Data retrieval from groundwater observations network is performed quarterly.

To identify and monitor the hydrogeochemical characteristics and the evolution of groundwater in the PHO, a groundwater quality–monitoring network was established, including the 12 stations (wells) of the basic observations network mentioned previously. Groundwater sampling was performed biannually: in late spring (before the start of irrigation period and at the end of recharge period) and in early autumn (after the end of irrigation period and before the end of dry season). In situ monitoring of pH, water temperature, EC, dissolved O_2, and oxidation–reduction potential was made using a YSI EXO2 multiparameter sonde. A wide range of hydrogeochemical parameters were determined in the accredited (after ELOT EN ISO/IEC 17025) laboratory of Soil and Water Resources Institute, including major and minor cations (K^+, Na^+, Ca^{2+}, Mg^{2+}, NH_4^+), anions (Cl^-, HCO_3^-, SO_4^{2-}, and NO_3^-), and heavy metals/metalloids (B, Cu, Zn, Fe, Mn, Pb, Ni, Cd, Cr, As, Hg). Until now, two groundwater sampling surveys had been conducted (25 May 2017 and 19 Oct. 2017).

Data Management And Policy

Data collected with sensors installed at the PHO are made publicly available via the Sensor Observation Service of the distributed spatial data infrastructure TEODOOR (Kunkel et al., 2013) at https://deos-id.org:8000/20.500.11952/DEOS/PHO. Before being published, data undergo a quality-checking procedure in which each dataset gets assigned a quality flag as described in Devaraju et al. (2015). The TEODOOR data portal was developed in the framework of the Terrestrial Environmental Observatories (TERENO) initiative (Zacharias et al., 2011) and is described in more detail in Bogena et al. (2018). In response to the needs expressed by the local farmers for easy-to-comprehend visualized results of the climate station monitoring and in accordance with Motive 7, a fact sheet for each climate station of the last 14-d evolution of key meteorological parameters, along with a time-stamped set of measured values with a time lag of ∼4 h, is made available through the following links that are communicated to the regional society: CS1, https://deos-id.org:8000/20.500.11952/ DEOS.MEDINET/00000708; CS2, https://deos-id. org:8000/20.500.11952/DEOS.MEDINET/00000709; CS3, https://deos-id.org:8000/20.500.11952/DEOS. MEDINET/1056009574.

Preliminary Scientific Findings and Insights

Evaluation of Data from Precipitation and Climate Observation Devices

The most common approach implemented in water balance models for determining ETo is based on the Penman–Monteith equation (Allen et al., 1994; Monteith, 1965). However, this approach requires four observed climatic variables: near-surface air temperature, humidity, wind speed, and net solar radiation. The Hargreaves equation (Hargreaves and Samani, 1985) provides a good approximation of ETo using temperature as the only (observed) climate variable, whereas the second variable (i.e., solar radiation) is taken into account by calculated (theoretical) values of extraterrestrial radiation at the top of the atmosphere. Therefore, the Hargreaves equation is often applied in regions where available climate data are sparse.

In many regions, a bias remains when ETo values from the Hargreaves equation are compared with those obtained with the Penman–Monteith approach. Consequently, Allen et al. (1998) recommend correcting these biases whenever possible. In recent studies, significant effort has been made to recalibrate the Hargreaves equation and to implement altitudinal gradients of mountainous terrains into gridding algorithms for the computation of ETo fields (e.g., Aguilar and Polo, 2011; Feng et al., 2017; Haslinger and Bartsch, 2016).

Contributing to Motives 1, 2, and 4 and after 1 yr (1 May 2017 to 30 Apr. 2018) of simultaneous operation of CS1 (located in the plain of PHO at 113 m asl) and CS3 (located in the mountains north of the PHO at 1033 m asl), the relation between ground surface altitude and measured climatic parameters has been analyzed preliminarily. Figure 3 shows the monthly statistics of altitudinal gradients of daily ETo fields from the Penman–Monteith equation (upper left) and from the Hargreaves equation (upper right). Both graphs show the highest decrease of ETo with altitude during summer, whereas the curves drawn by monthly median gradients (bold lines in boxes) take different courses. Thus, daily ETo gradients from both equations differ not only in their total amount and annual cycle also in that the bias of the Hargreaves approach varies with the altitude level. This fact should be considered when implementing the gridding procedure for ETo in the whole RPB domain.

In meteorology, the "lapse rate" is the rate at which air cools with elevation change. The adiabatic lapse rate (i.e., no heat exchange) varies between −0.98 K per 100 m (dry) and −0.4 K per 100 m (saturated). Due to several processes (e.g., evaporation or condensation of moisture, advection of air masses, and heating or cooling at the surface), lapse rates can be regarded as predominantly nonadiabatic. In this case they are designated as environmental lapse rates (Barry and Chorley, 1987; Dodson and Marks, 1997). Average global (environmental) lapse rates referred to in the literature range from −0.55 to −0.65 K per 100 m. They are assumed to represent rough approximations and are therefore not recommended for precise modeling studies (Rolland, 2003). The calculation of environmental lapse rates in the PHO is constrained by two altitude levels. To be consistent with the term "altitudinal gradients of ETo," we term environmental lapse rates here as "altitudinal gradients of temperature." The statistics of temperature gradients indirectly influence the statistics of ETo gradients.

Figure 3 shows the statistics of altitudinal gradients of the daily minimum (lower left) and maximum (lower right) near-surface minimum and maximum air temperature (Tmin and Tmax, respectively). The median gradients of Tmax are in quite good agreement with the average global (environmental) lapse rates stated above, whereas the median gradients of Tmin show a contrary pattern. This might be caused by nocturnal mountain-valley winds (i.e., the orographic upslope flow of air masses that regularly heat up over the wider PHO plain area and the eastern Thessaly plain during the days with positive radiation balance; details in Pielke [1984]). These air masses rise up in the mountain range and therefore increase measured Tmin at higher altitude over night. The comparatively large range of Tmin gradients from positive to negative is caused by the frequently varying atmospheric instability. Also, temperature inversions occur regularly. In addition to the relevance of temperature gradients in the computation of ETo fields, the gradients presented here are intended to be used in the mGROWA model for adjusting the temperature index–based snowpack module.

Evaluation of Soil Water Content Observations for First Period Observation Year

Figure 4 illustrates preliminary results from the first observation year (May 2017 to March 2018). During this period, we
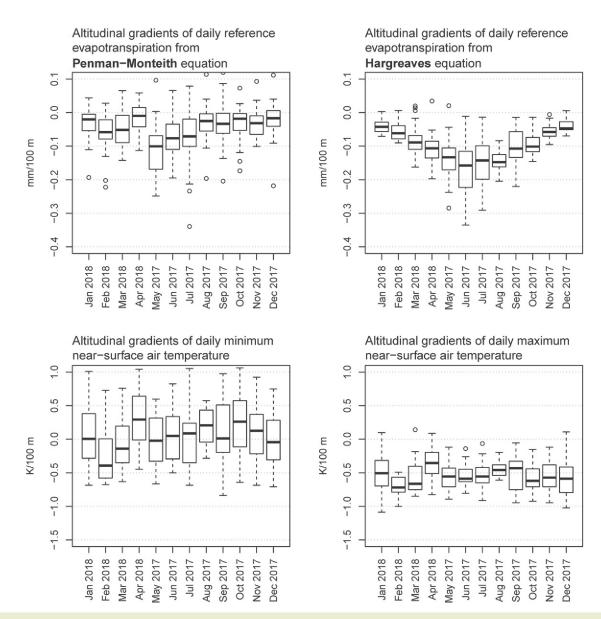
Fig. 3. Altitudinal gradients of reference evapotranspiration and near-surface air temperature based on measurements at climate stations CS1 and CS3 (at 113 and 1033 m asl).

observed 1233 mm of precipitation, with maximum rainfall intensities of 111 mm d^{-1}. The average air temperature was 12.3°C (range, −2.5 to 30.6°C). During the winter, three distinctive snow events occurred in which the maximum snow depths ranged between 20 and 45 cm. Soil moisture, as measured by the SoilNet nodes, varied during the year at 5 cm depth from 0.05 to 0.29 cm^3 cm^{-3} (average, 0.16 cm^3 cm^{-3}) and at 50 cm depth from 0.12 to 0.39 cm^3 cm^{-3} (average, 0.24 cm^3 cm^{-3}). Figure 4 shows the average soil moisture at all depths. A strong soil moisture response was observed especially during the summer after intensive precipitation events. The temporal resolution of the soil moisture determined by the CRNS probes is 1 d, and no smoothing was applied. These values coincide very well with the average SoilNet data (RMSE, 0.033 cm^3 cm^{-3}).

Systematic deviations can be observed during the summer and winter periods. The former might be explained by the influence

of biomass (e.g., Baatz et al., 2015; Jakobi et al., 2018) or by stronger gradients in the soil profile after precipitation events because SoilNet measurements start at 5 cm, whereas the CRNS probe is most sensitive to the first 1 cm in the soil (Jakobi et al., 2018). The latter can be explained by the occurrence of snow covers. Because snow contains hydrogen, the fast neutron count rate drastically decreases, leading to overestimation of soil moisture in winter (Schattan et al., 2017). The above results demonstrate the potential of the PHO to be used as a testing facility for soil moisture–monitoring sensors, thus contributing to Motive 8.

After some seasons in operation, the soil moisture data are intended to serve as a storage term in the framework of calibration of mGROWA parameters with relation of ET fluxes emerging by Mediterranean scrubland. Because ET is not measured directly in the PHO, ET time series will be derived using the water balance equation (i.e., from precipitation, total soil water storage capacity,
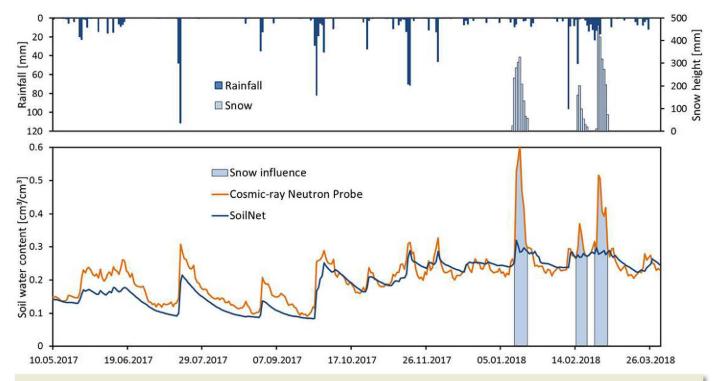
Fig. 4. Rainfall, snow depth, and soil water content measured from May 2017 to March 2018 at the soil moisture observation site at 1033 m asl (CS3). The rain gauge had a malfunction during the first snow event in January 2018.

and rooting zone determined from laboratory and in situ analysis) and the measured fluctuation patterns of soil moisture.

Conceptualization of Water Balance and Evaluation of Data from Groundwater Observation Devices

There is a wide range of methods and equations applied for water balance representation, ranging from the simple form to more complex and comprehensive approaches, such as that of Li et al. (2018). Regarding Motives 3 and 5, a simplified version of water balance has been adopted that focuses on the basin fluxes, according to the zones demonstrated in Fig. 5:

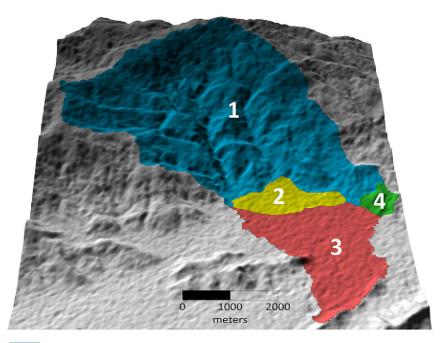$$\sum P_i + LI_3 = \sum ET_i + \sum TR_i + GA_2 + GA_3 + LO_3 \qquad [1]$$

where i is the water balance zone number, P is precipitation, LI is lateral groundwater inflow, ET is evapotranspiration, TR is the total runoff (direct runoff and baseflow), GA is groundwater abstractions, and LO is lateral groundwater outflow.

Zone 1 includes fractured formations (mainly gneiss and gneiss-schists) in which there are no groundwater abstractions and lateral inflows or outflows. Therefore, the TR and ET constitute the only outflows from Zone 1 because it is hydrologically and hydrogeologically isolated. Given that two meteorological stations are installed in this zone, P is efficiently monitored. Moreover, the results of the snow depth sensor are expected to give significant insight to the contribution of snow to the water balance. Regarding ET, the SoilNet clusters and CNRS sensor accompanied by meteorological data and modeling are expected

to give significant information about the crop coefficient factor of the native vegetation on the mountainous areas and therefore approach ET calculation more efficiently. Considering that P and ET are satisfactorily measured and calculated, TR can be simulated using the fully distributed mGROWA model.

Total runoff from Zone 1 is transferred to Zone 2, comprising of old scree cones and screes, which form the core of the transition zone. Except for ET, which is the main outflow from Zone 2, groundwater abstractions to satisfy irrigation needs have to be considered. The latter are satisfactorily monitored through water abstraction loggers, which will provide insight about irrigation practices not only for Zone 2 but also for Zone 3. Moreover, the SoilNet installed in Zone 2 will give information not only for irrigation practices effects in soil water balance but also about groundwater recharge in the transition zone (through modeling), and therefore it will provide insight about total runoff separation in the transition zone as simulated with mGROWA. The groundwater-level monitoring network in Zone 2, accompanied by all the above, will give the appropriate data for the development of a groundwater flow model in the transition zone that will provide new evidence about its hydrologic behavior.

Total runoff from the transition zone (Zone 2) is transferred to Zone 3, which is developed within the alluvial deposits of the plain area. In addition to precipitation, ET, and TR, lateral groundwater inflows and outflows have to be taken into account in the water balance because Zone 3 is not hydrogeologically isolated. Precipitation and the meteorological parameters assisting ET calculation with the Penman–Monteith method are adequately monitored in CS1. Actual groundwater abstractions monitoring in the five key points

1   Fractured-weathered formations, no groundwater abstractions and lateral inflows or outflows

2   Transition zone, inflows from zone 1 and outflows to zone 3, groundwater abstractions

3   Alluvial deposits, significant groundwater abstractions and inflows from zone 2

4   Serpentines and limited karstic formations, small contribution of inflows to zone 3

in Zone 3 will give significant information about the actual groundwater abstractions for irrigation. Groundwater level accompanied by TR simulation with mGROWA will assist the development of a groundwater flow model, which will further give information about the alluvial aquifer and its lateral hydraulic interactions.

Zone 4 covers a small part of the PHO and consists mainly of serpentines of very low to low permeability, accompanied by karstic formations of limited size. Zone 4 is not hydrologically connected to the transition zone, but it is expected to have a very small contribution to the alluvial aquifer in Zone 3.

Relying on data retrieved from groundwater level–monitoring stations, the spatial distributions of groundwater level for April and October 2017 were produced and are presented in Fig. 6. April was selected because it is representative of the maximum groundwater level distribution corresponding to the end of the wet period, just before initiation of irrigation. In a similar way, October was selected as representative of the minimum groundwater level distribution corresponding to the end of the dry period, just after the end of irrigation. The common characteristics of groundwater level distribution for both periods are (i) higher hydraulic slopes are observed in the transition zone (HP4 unit), which become milder to the south within the alluvial deposits, and (ii) the general groundwater flow direction remains constant from northwest to the southeast. To more clearly identify changes in groundwater level spatial distribution, a third map (Fig. 6c) was produced presenting groundwater level change between October and April 2017. Studying this map,

more complex groundwater level change patterns are revealed in the northern half of the transition zone ranging from 1.4 to 6 m. Groundwater level change becomes more uniform in the alluvial deposits. On average, and for both hydrolithological units, groundwater level change was 2.8 m. By calculating the volume included between the two groundwater level surfaces and assuming an average effective porosity value of 10% on the basis of literature referring to similar alluvium deposits in the wider region (Alexandridis et al., 2014; Panagopoulos, 1995), groundwater losses during the period April to October 2017 (including irrigation and hydraulic interaction gains and losses in the alluvial deposits) was estimated at 2.8 Mm^3 or about 290 mm.

Regarding groundwater quality, the descriptive statistics of physicochemical parameters monitored through the two groundwater sampling surveys performed in 2017 are summarized in Table 2. Based on the median values of the measured variables, groundwater is circumneutral (7.3), and EC is 508 µS cm^{-1}, indicating good quality for irrigation water. The dominant cation in groundwater is Ca^{2+}, followed by Mg^{2+} and Na$^+$, in descending order. The dominant anion in groundwater is HCO$_3^-$, followed by NO$_3^-$ and Cl$^-$. The presence of nitrates among the dominant anions is indicative of the anthropogenic impact due to agricultural activities; however, its median concentration is relatively low (17 mg L^{-1}), and the impact is mainly observed locally (concentrations up to 86.5 mg L^{-1}). The concentrations of heavy metals/metalloids are low and fall within the typical margins of natural groundwaters (Hem, 1985). No significant variations were observed among the
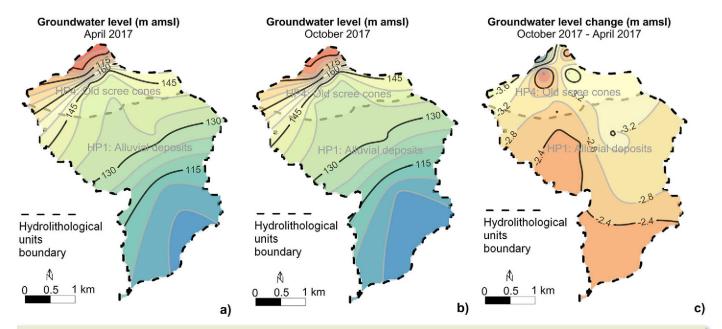
Fig. 6. Spatial distribution of the average groundwater level for the southern part of the Pinios Hydrologic Observatory (PHO) watershed (hydrolithological formations HP1 and HP4) on (a) April 2017 and (b) October 2017, and (c) groundwater level change between these periods.

Table 2. Descriptive statistics of groundwater samples ($n = 12$).

Variable	LOQ†	25 May 2017 Median	19 Oct. 2017 Median	All periods SD	Min.	Median	Max.
pH	3–10	7.3	7.3	0.2	7.0	7.3	7.7
EC,‡ $\mu S\,cm^{-1}$	0.7	539	508	149	324	508	986
K^+, $mg\,L^{-1}$	1	1.2	1.1	0.4	0.5	1.2	2.1
Na^+, $mg\,L^{-1}$	1	11.2	10.2	2.8	5.3	11.1	17.0
Ca^{2+}, $mg\,L^{-1}$	2.6	94.4	84	26.4	58.5	86.8	162.5
Mg^{2+}, $mg\,L^{-1}$	0.8	18.7	18.2	4.8	7.3	18.4	25.7
HCO_3^-	–	292	281	80.5	179	287	574
Cl^-, $mg\,L^{-1}$	0.5	13.6	12.8	5.7	8.0	13.0	33.2
SO_4^{2-}, $mg\,L^{-1}$	–	2.1	14.5	18.7	0.5	5.9	73.5
NO_3^-, $mg\,L^{-1}$	–	17.8	18.8	19.1	1.0	17.0	86.5
NH_4^+, $mg\,L^{-1}$	–	0.1	0.1	0.2	0	0.1	0.9
B, $\mu g\,L^{-1}$	52	10	17	20	0	14	79
Cu, $\mu g\,L^{-1}$	100	0.5	0.4	1.7	0	0.4	8.1
Fe, $\mu g\,L^{-1}$	10	22.2	15.5	16.4	1.3	17.7	86.5
Mn, $\mu g\,L^{-1}$	6.5	1.0	1.5	6.2	0.5	1.3	31.3
Ni, $\mu g\,L^{-1}$	5	0.6	1.9	1.9	0	1.4	8.0
Cd, $\mu g\,L^{-1}$	0.3	0	0.1	0.1	0	0	0.3
Cr, $\mu g\,L^{-1}$	2	1.8	2.1	2.1	0	1.6	8.6
As, $\mu g\,L^{-1}$	1	0.3	0.6	0.7	0	0.5	2.7
Zn, $\mu g\,L^{-1}$	200	35	26	39	17	27	183
Hg, $\mu g\,L^{-1}$	1	0	0	0	0	0	0
Pb, $\mu g\,L^{-1}$	5	0	0	0	0	0	0

† Limit of quantification.
‡ Electrical conductivity.

two sampling periods. Nevertheless, sulfates are rather low in the first period, probably indicating a temporal reducing environment affecting their concentration.

All groundwater samples have the same water type (Ca-HCO_3), which is evident from their common hydrodynamic characterization, which classifies them as recharge waters. Their common hydrogeochemical signature is also clearly identified in the Piper diagram in Fig. 7. These observations are in line with the geological and hydrogeological regime of the PHO, confirming that the area constitutes a recharge window, where the lateral crossflows from the metamorphic bedrock recharges the alluvium plain through a general north–south direction. Along the same direction, EC values and NO_3^- concentrations increase with distance from the transition zone. Hence, EC values vary from 0.49 to 0.62 mS cm^{-1} and NO_3^- concentrations from 8.8 to 31.5 mg L^{-1}, which may suggest the contribution of pristine water quality lateral crossflows from the transition zone to the alluvial groundwater system.

Based on the calculated saturation indices ($\log Q/K$) for the main mineral phases expected, calcite and dolomite are oversaturated in all samples; hence, these phases are the main precipitates that are deposited in the aquifer matrix. The molar ratios of Ca/HCO_3 of all samples are <0.5 (range 0.28–0.38). Considering the overall geological regime, the primary source of calcium is possibly attributed to the ion exchange process (Hounslow, 1995; Tziritis et al., 2016). Specifically, Na^+, which is enriched in solute due to metamorphic rocks, exchanges with Ca^{2+}, which is hosted in Ca-rich feldspars such as anorthite ($CaAl_2Si_2O_8$). This process also explains the relatively low Na^+ concentrations in groundwater, contradictory to those expected according to bedrock geology. Calcium may also originate from the weathering of Ca-rich silicate minerals (e.g., diopsidic pyroxene [$CaMgSi_2O_6$]), which are
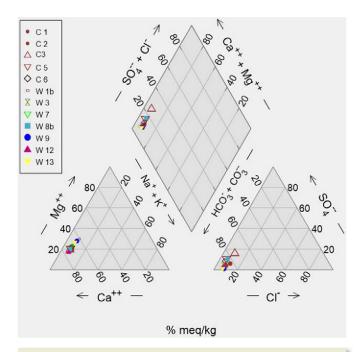
Fig. 7. Piper diagram for groundwater samples (average values of two periods).

abundant in the metamorphic bedrock. Indeed, in-depth investigation of regional hydrogeochemistry to decipher prevalent evolution mechanisms is among the research fields currently being developed in the PHO.

The average daily variation of EC and groundwater level on the three groundwater wells equipped with conductivity, temperature, and depth sensors (C5, W9, and W13) (Fig. 1d) are presented in Fig. 8. Whereas EC variation for W13 is low ($\sim$40 μS cm^{-1}), the variation for the other two monitoring points is much higher; the highest variation was observed at C5 and was observed mainly during the irrigation period. Monitoring station W13 is the furthest upstream monitoring well of our network and hence is mostly influenced by fresh recharge surges from the mountainous region through the transition zone and receives the least pressure from imposed agricultural activities. Monitoring station W9 is also located within the transition zone but further downstream compared with W13. Therefore, resident groundwater along with recharge water mounds control groundwater chemistry at that zone. Monitoring station C5 is located at the plain and close to the end point members of the alluvial groundwater system. Hence, hydrogeochemical evolution at C5 is mostly controlled by resident groundwater that is influenced predominantly by practiced activities on topsoil and by the mineralogy of the aquifer matrix. In addition to these observations, the observed variations and differences between the three monitoring points may be attributed to (i) abstractions from different aquifer layers as the groundwater level is falling during the irrigation period and (ii) the leaching and remobilization of precipitated salts in the aquifer matrix. The latter is a process that occurs naturally with regular groundwater flow; nevertheless, it is a relatively slow process and depends on groundwater velocity. During the irrigation period,

pumping may trigger elevated groundwater fluxes, thus enhancing the naturally occurring process of leaching and resulting in increased EC values. However, the impact is local and cannot be generalized to the entire groundwater system. This is also supported by the fact that higher EC increments are observed in boreholes that abstract higher volumes of groundwater (based on irrigation needs), whereas in boreholes, whose abstraction is significantly lower, the EC values are practically constant. Another interesting observation from the high-frequency conductivity, temperature, and depth measurements on these boreholes is that EC variations exhibit an hourly pattern in most cases coincide with pumping times. This observation is in line with the seasonal variation exhibited and demonstrates the potential of high-frequency monitoring for giving new insight about hydrogeochemical processes taking place in the aquifer with respect to Motive 5. In fact, EC variations are inversely proportional to groundwater level fluctuation.

Based on hydrogeochemical assessments, the composition of the leached precipitates should be dominated by calcite and dolomite, both being oversaturated to groundwater solute. The leaching of accumulated salts (or fertilizers) on the topsoil due to the applied irrigation water should be excluded because in that case a defined time-lag between EC increment and irrigation water application should exist. On the contrary, the EC variations triggered almost coincide with the irrigation period, leading to the conclusion that leaching and enrichment of solids in groundwater solute is an internal process that occurs in the saturated zone.

Future Perspectives

The PHO has already started yielding valuable information on the hydro-geo environment of the Agia basin. Its potential is high and will be exploited within the next years (i.e., under consideration of longer time series of the parameters assessed). Detailed calculation of hydrologic water balance based on the collected data is the top priority for future studies (Motives 3 and 5). Key water balance elements will be calculated in the immediate future on the basis of the collected and analyzed data. Hence, in addition to precipitation, which is accurately measured, and ETo, which is calculated using the standard Penman–Monteith equation (Allen et al., 1998), groundwater recharge will be closely approximated. The driving recharge mechanisms to the alluvial aquifer system have been identified based on the installed groundwater level sensors and the hydrochemical analyses and will be quantified in the near future using further methods of investigation, including isotope hydrology. Regarding Motive 4, appropriate transfer functions from the local to the regional scale regarding lateral crossflow description and quantification is the next step once the previously discussed calculations are adequately documented. This task will enhance the ongoing modeling exercise at the RPB by rectifying the defined hydrological budgeting elements of lateral crossflows.

Numerous data sets of short pumping tests have been recorded from the installed monitoring devices. These consist of high-frequency records of groundwater fluctuations and the corresponding
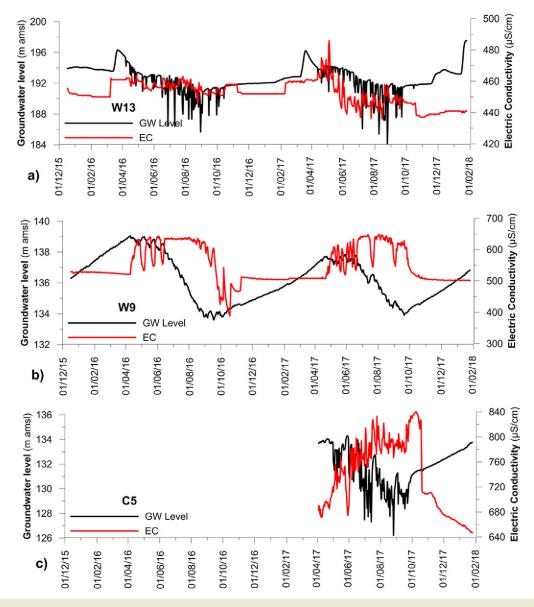
Fig. 8. Variation of average daily groundwater level and electric conductivity for monitoring stations W13, W9, and C5.

abstraction rates. Pressure transducers are installed in the production or in satellite wells. Additionally, EC values are recorded at three monitoring points. Available abstraction time series are rather short and vary from an hour during winter and springtime to a day in peak demand periods and hence are not representative of a pumping test analysis time series duration. A common shortcoming not only in the PHO and nationwide but in most basins is the lack of reliable data about hydraulic properties. Against this background and with respect to Motive 5, the PHO will be used as a case study area for the development of a robust methodology to analyze successive short-duration pumping test series with the aim to derive hydraulic properties and assess the efficiency of production wells. As the methodology is designed as an inexpensive but reliable alternative to expensive pumping tests for hydraulic property assessments and periodic review of well construction characteristics, its transfer to numerous basins across the globe is an ambitious but still realizable option.

Based on the experience gained so far, a three-fold expansion for the PHO is foreseen:

1. The soil monitoring network needs to be expanded to obtain better coverage of the entire test basin. This will include the installation of more SoilNet nodes and CRNS probes, thus contributing to Motives 1, 2, and 3. Conventional pedologic studies are planned to contribute to the knowledge gained for the basin and will include analysis of hydraulic soil properties, organic matter, and nutrients and micronutrients.

2. The groundwater monitoring network needs to be expanded and to incorporate surface water monitoring sites that are missing in the present installation set-up to increase the accuracy and decrease the uncertainty in water budgeting and hydrodynamic evolution research. Additional quality parameters will also be measured, including environmental isotopes, for further hydrodynamical and hydrogeochemical characterization. This expansion will provide better understanding and thus control of the system. All the above are contributing to the majority of our motives for PHO establishment.

3. Logging equipment must be converted to telemetric stations, and key water quality sensors must be installed. This will increase the potential of offering services to the community (Motive 7).

The overall target of this expansion is to initiate a distributed irrigation programming protocol that we envisage to fully implement in the entire area covered by the PHO. This will act as a pilot and subsequently as a demo basin for farmers and stakeholders involved in irrigation water management at regional and national scales. Irrigation management in the PHO is seen only as part of an integrated water resources management scheme, and such schemes are only successful if applied at local scales where an active, participatory approach is adopted and practiced. Hence, a key future perspective for the PHO is to develop water governance strategies for effective water management based on decision support tools driven by the network and models and the active participation of local stakeholders (Motives 6 and 8).

The PHO offers a challenging environment for the entire spectrum of environmental sciences and socioeconomics. As such, it will be expanded as a multidisciplinary scientific forum for researchers to work on by testing methodologies for advanced analysis, hydrologic models, sensors, and instruments, thus contributing to Motives 5 and 8. Furthermore, being a field laboratory, academics and students have begun to study the PHO for undergraduate and postgraduate theses. This is a function we are keen to establish and expand, offering in cooperation with environmental agencies and environmental education groups and customized programs of scientific information/training for every level of education (primary, secondary, and academic).

References

Aguilar, C., and M.J. Polo. 2011. Generating reference evapotranspiration surfaces from the Hargreaves equation at watershed scale. Hydrol. Earth Syst. Sci. 15:2495–2508. doi:10.5194/hess-15-2495-2011

Alexandridis, T.K., A. Panagopoulos, G. Galanis, I. Alexiou, Y. Cherif, Y. Chemin, et al. 2014. Combining remotely sensed surface energy fluxes and GIS analysis of groundwater parameters for irrigation system assessment. J. Irrig. Sci. 32:127–140. doi:10.1007/s00271-013-0419-8

Allen, R.G., L.S. Pereira, D. Raes, and M. Smith. 1998. Crop evapotranspiration: Guidelines for computing crop water requirements. FAO, Rome.

Allen, R.G., M. Smith, A. Perrier, and L.S. Pereira. 1994. An update for the definition of reference evapotranspiration. ICID Bull. 43:1–34.

Andreasen, M., K.H. Jensen, D. Desilets, T.E. Franz, M. Zreda, H.R. Bogena, and M.C. Looms. 2017. Status and perspectives on the cosmic-ray neutron method for soil moisture estimation and other environmental science applications. Vadose Zone J. 16(8). doi:10.2136/vzj2017.04.0086

Baatz, R., H.R. Bogena, H.J. Hendricks Franssen, J.A. Huisman, C. Montzka, and H. Vereecken. 2015. An empirical vegetation correction for soil water content quantification using cosmic ray probes. Water Resour. Res. 51:2030–2046. doi:10.1002/2014WR016443

Bangash, R.F., A. Passuello, M. Sanchez-Canales, M. Terrado, A. López, F.J. Elorza, et al. 2013. Ecosystem services in Mediterranean river basin: Climate change impact on water provisioning and erosion control. Sci. Total Environ. 458–460:246–255. doi:10.1016/j.scitotenv.2013.04.025

Barry, R.G., and R.J. Chorley. 1987. Atmosphere, weather and climate. 5th ed. Routledge, London.

Bogena, H.R., M. Herbst, J.A. Huisman, U. Rosenbaum, A. Weuthen, and H. Vereecken. 2010. Potential of wireless sensor networks for measuring soil water content variability. Vadose Zone J. 9:1002–1013. doi:10.2136/vzj2009.0173

Bogena, H.R., J.A. Huisman, A. Güntner, C. Hübner, J. Kusche, F. Jonard, et al. 2015. Emerging methods for noninvasive sensing of soil moisture dynamics from field to catchment scale: A review. Wiley Interdiscip. Rev.: Water 2:635–647. doi:10.1002/wat2.1097

Bogena, H., J. Huisman, B. Schilling, A. Weuthen, and H. Vereecken. 2017. Effective calibration of low-cost soil water content sensors. Sensors 17:208. doi:10.3390/s17010208

Bogena, H.R., C. Montzka, J.A. Huisman, A. Graf, M. Schmidt, M. Stockinger, et al. 2018. The TERENO-Rur Hydrological Observatory: A multi-scale multi-compartment research platform for the advancement of hydrological science. Vadose Zone J. 17:180055. doi:10.2136/vzj2018.03.0055

Chenoweth, J., P. Hadjinicolaou, A. Bruggeman, J. Lelieveld, Z. Levin, M.A. Lange, et al. 2011. Impact of climate change on the water resources of the eastern Mediterranean and Middle East region: Modeled 21st century changes and implications. Water Resour. Res. 47:W06506. doi:10.1029/2010WR010269

Desilets, D., M. Zreda, and T.P.A. Ferré. 2010. Nature's neutron probe: Land surface hydrology at an elusive scale with cosmic rays. Water Resour. Res. 46:W11505. doi:10.1029/2009WR008726

Devaraju, A., S. Jirka, R. Kunkel, and J. Sorg. 2015. Q-SOS: A sensor observation service for accessing quality descriptions of environmental data. ISPRS Int. J. Geo-Inf. 4:1346–1365. doi:10.3390/ijgi4031346

Dodson, R., and D. Marks. 1997. Daily air temperature interpolated at high spatial resolution over a large mountainous region. Clim. Res. 8:1–20. doi:10.3354/cr008001

Ehlers, L., F. Herrmann, M. Blaschek, R. Duttmann, and F. Wendland. 2016. Sensitivity of mGROWA-simulated groundwater recharge to changes in soil and land use parameters in a Mediterranean environment and conclusions in view of ensemble-based climate impact simulations. Sci. Total Environ. 543:937–951. doi:10.1016/j.scitotenv.2015.04.122

Feng, Y., Y. Jia, N. Cui, L. Zhao, C. Li, and D. Gong. 2017. Calibration of Hargreaves model for reference evapotranspiration estimation in Sichuan basin of southwest China. Agric. Water Manage. 181:1–9. doi:10.1016/j.agwat.2016.11.010

García-Ruiz, J.M., J.I. López-Moreno, S.M. Vicente-Serrano, T. Lasanta-Martínez, and S. Beguería. 2011. Mediterranean water resources in a global change scenario. Earth Sci. Rev. 105:121–139. doi:10.1016/j.earscirev.2011.01.006

Hargreaves, G.H., and Z.A. Samani. 1985. Reference crop evapotranspiration from temperature. Appl. Eng. Agric. 1:96–99. doi:10.13031/2013.26773

Haslinger, K., and A. Bartsch. 2016. Creating long-term gridded fields of reference evapotranspiration in Alpine terrain based on a recalibrated Hargreaves method. Hydrol. Earth Syst. Sci. 20:1211–1223. doi:10.5194/hess-20-1211-2016

Hellenic Ministry of Agricultural Development and Food. 2012. Preliminary engineering and geological study for the construction of a reservoir in the Prefecture of Larissa, Agiokampos "Livadotopos" site, Athens. Ministry of Agricultural Development and Food, Athens, Greece.

Hellenic Special Secretariat for Water. 2012. Compilation of management plans for the river basins of the water districts of Thessaly, Epirus and western Sterea Hellas in accordance to Directive 2000/60/EC and in implementation of A. 3199/2003 and PD 51/2007: Water Management Plan—Water District of Thessaly. Ministry of Environment, Energy and Climate Change, Special Secretariat for Water, Athens, Greece.

Hellenic Special Secretariat for Water. 2017. First review of river basin

management plan of Thessaly Water District (EL08). Ministry for the Environment, Energy and Climate Change, Athens, Greece.

Hem, J. 1985. Study and interpretation of the chemical characteristics of natural water. Water-Supply Pap. 2254. USGS, Reston, VA.

Herrmann, F., N. Baghdadi, M. Blaschek, R. Deidda, R. Duttmann, I. La Jeunesse, et al. 2016. Simulation of future groundwater recharge using a climate model ensemble and SAR-image based soil parameter distributions: A case study in an intensively-used Mediterranean catchment. Sci. Total Environ. 543:889–905. doi:10.1016/j.scitotenv.2015.07.036

Herrmann, F., L. Keller, R. Kunkel, H. Vereecken, and F. Wendland. 2015. Determination of spatially differentiated water balance components including groundwater recharge on the Federal State level: A case study using the mGROWA model in North Rhine-Westphalia (Germany). J. Hydrol.: Regional Stud. 4:294–312. doi:10.1016/j.ejrh.2015.06.018

Hounslow, A.W. 1995. Water quality data: Analysis and interpretation. CRC Press, Boca Raton, FL.

Jakobi, J., J.A. Huisman, H. Vereecken, B. Diekkrüger, and H.R. Bogena. 2018. Cosmic-ray neutron sensing for simultaneous soil water content and biomass quantification in drought conditions. Water Resour. Res. doi:10.1029/2018WR022692

Kaplanidis, A., and D. Fountoulis. 1997. Subsidence phenomena and ground fissures in Larissa, Karla basin, Greece: Their results in urban and rural environment. In: P.G. Marinos et al., editors, Proceedings of International Symposium on Engineering Geology and the Environment, 23–27 June 1997, Athens, Greece. Vol. 1. A.A. Balkema, Rotterdam, the Netherlands. p. 729–735.

Karyotis, T., A. Panagopoulos, D. Pateras, A. Panoras, N. Danalatos, C. Angelakis, and C. Kosmas. 2002. The Greek Action Plan for the mitigation of nitrates in water resources of the vulnerable district of Thessaly. J. Mediterr. Ecol. 3:77–83.

Köhli, M., M. Schrön, M. Zreda, U. Schmidt, P. Dietrich, and S. Zacharias. 2015. Footprint characteristics revised for field-scale soil moisture monitoring with cosmic-ray neutrons. Water Resour. Res. 51:5772–5790. doi:10.1002/2015WR017169

Koukidou, I., and A. Panagopoulos. 2010. Application of FEFLOW for the simulation of groundwater flow at the Tirnavos (central Greece) alluvial basin aquifer system. Bull. Geol. Soc. Greece 43:1747–1757. doi:10.12681/bgsg.11360

Kunkel, R., J. Sorg, R. Eckardt, O. Kolditz, K. Rin, and H. Vereecken. 2013. TEODOOR: A distributed geodata infrastructure for terrestrial observation data. Environ. Earth Sci. 69:507–521. doi:10.1007/s12665-013-2370-7

Kunkel, R., and F. Wendland. 2002. The GROWA98 model for water balance analysis in large river basins: The River Elbe case study. J. Hydrol. 259:152–162. doi:10.1016/S0022-1694(01)00579-0

Li, X., G. Cheng, Y. Ge, H. Li, F. Han, X. Hu, et al. 2018. Hydrological cycle in the Heihe River basin and its implication for water resource management in endorheic basins. J. Geophys. Res.: Atmos. 123:890–914. doi:10.1002/2017JD027889

Marinos, P., M. Kavvadas, and V. Perleros. 1997. Investigation of the over-exploitation of a major alluvial aquifer in Thessaly, Greece. In: J.D. Powell, editor, Proceedings of 3rd USA/CIS joint conference on environmental hydrology and hydrogeology: Water sustaining a critical resource: A selection of papers presented by hydrologists, Tashkent, Uzbekistan. 22–27 Sept. 1996. Am. Inst. Hydrol., St. Paul, MN. p. 29–38.

Milano, M., D. Ruelland, S. Fernandez, A. Dezetter, J. Fabre, E. Servat, et al. 2013. Current state of Mediterranean water resources and future trends under climatic and anthropogenic changes. Hydrol. Sci. J. 58:498–518. doi:10.1080/02626667.2013.774458

Mirtl, M., E.T. Borer, I. Djukic, M. Forsius, H. Haubolda, W. Hugo, et al. 2018. Genesis, goals and achievements of long-term ecological research at the global scale: A critical review of ILTER and future directions. Sci. Total Environ. 626:1439–1462. doi:10.1016/j.scitotenv.2017.12.001

Monteith, J.L. 1965. Evaporation and environment. Symp. Soc. Exp. Biol. 19:205–234.

Panagopoulos, A. 1995. A methodology for groundwater resources management of a typical alluvial aquifer system in Greece. Ph.D. diss. Univ. of Birmingham, Birmingham, UK.

Panagopoulos, A. 1996. Groundwater resources management study of the Tyrnavos alluvial basin using mathematical models. In: Proceedings of the 2nd PanHellenic Conference on Land Reclamation Works and Water Resources Management, Larissa, Greece. p. 393–404.

Panagopoulos, A., G. Arampatzis, P. Kuhr, R. Kunkel, E. Tziritis, and F. Wendland. 2015. Area-differentiated modeling of water balance in Pinios Basin, central Greece. Global NEST J. 17:221–235. doi:10.30955/gnj.001402

Panagopoulos, A., G. Arampatzis, E. Tziritis, V. Pisinaras, F. Herrmann, R. Kunkel, and F. Wendland. 2016. Assessment of climate change impact in the hydrological regime of River Pinios basin, central Greece. Desalin. Water Treat. 57:2256–2267. doi:10.1080/19443994.2014.984926

Panagopoulos, A., F. Herrmann, V. Pisinaras, and F. Wendland. 2017. Impact of climate change on irrigation need and groundwater resources in Pinios Basin. Eur. Water 59:91–98.

Pielke, R.A. 1984. Mesoscale meteorological modeling. Academic Press, San Diego.

Pikounis, M., E. Varanou, E. Baltas, A. Dassaklis, and M. Mimikou. 2003. Application of the SWAT model in the Pinios River basin under different land-use scenarios. Glob. NEST J. 5(2):71–79.

Psomas, A., V. Dagalaki, Y. Panagopoulos, D. Konsta, and M. Mimikou. 2016. Sustainable agricultural water management in Pinios River basin using remote sensing and hydrologic modeling. Procedia Eng. 162:277–283. doi:10.1016/j.proeng.2016.11.059

Rolland, C. 2003. Spatial and seasonal variations of air temperature lapse rates in alpine regions. J. Climate 16:1032–1046. doi:10.1175/1520-0442(2003)016

Roson, R., and M. Sartori. 2010. Water scarcity and virtual water trade in the Mediterranean. IEFE Working Paper 38. SSRN, Rochester, NY. doi:10.2139/ssrn.1683290

Schattan, P., G. Baroni, S.E. Oswald, J. Schöber, C. Fey, C. Kormann, et al. 2017. Continuous monitoring of snowpack dynamics in alpine terrain by aboveground neutron sensing. Water Resour. Res. 53:3615–3634. doi:10.1002/2016wr020234

Schrön, M., M. Köhli, L. Scheiffele, J. Iwema, H.R. Bogena, L. Lv, et al. 2017. Improving calibration and validation of cosmic-ray neutron sensors in the light of spatial sensitivity: Theory and evidence. Hydrol. Earth Syst. Sci. 21:5009–5030. doi:10.5194/hess-2017-148

Tetzlaff, B., M. Andjelov, P. Kuhr, J. Uhan, and F. Wendland. 2015. Model-based assessment of groundwater recharge in Slovenia. Environ. Earth Sci. 74:6177–6192. doi:10.1007/s12665-015-4639-5

Tziritis, E., K. Skordas, and A. Kelepertzis. 2016. The use of hydrogeochemical analyses and multivariate statistics for the characterization of groundwater resources in complex aquifer system: A case study in Amyros River basin, Thessaly, central Greece. Environ. Earth Sci. 75:339. doi:10.1007/s12665-015-5204-y

Zacharias, S., H. Bogena, L. Samaniego, M. Mauder, R. Fuß, T. Puetz, et al. 2011. A network of terrestrial environmental observatories in Germany. Vadose Zone J. 10:955–973. doi:10.2136/vzj2010.0139

Zreda, M., W.J. Shuttleworth, X. Zeng, C. Zweck, D. Desilets, T. Franz, and R. Rosolem. 2012. COSMOS: The COsmic-ray Soil Moisture Observing System. Hydrol. Earth Syst. Sci. 16:4079–4099. doi:10.5194/hess-16-4079-2012